JOURNAL OF VIROLOGY, Dec. 1995, p. 7529–7540 Vol. 69, No. 12
0022-538X/95/$04.00+0

Function of a 5′-End Genomic RNA Mutation That Evolves during Persistent Mouse Hepatitis Virus Infection In Vitro

WAN CHEN AND RALPH S. BARIC*

Program in Infectious Diseases, Department of Epidemiology and Department of Microbiology and Immunology, University of North Carolina at Chapel Hill, Chapel Hill, North Carolina 27599-7400

Received 17 March 1995/Accepted 23 August 1995

Persistently infected cultures of DBT cells were established with mouse hepatitis virus strain A59 (MHV-A59), and the evolution of the MHV leader RNA and 5′ end of the genome was studied through 119 days postinfection. Sequence analysis of independent clones demonstrated an overall mutation frequency approaching 1.2×10^{-3} to 6.7×10^{-3}. The rate of fixation of mutations was about 1.2×10^{-5} to 7.6×10^{-5} per nucleotide (nt) per day. In contrast to finding in bovine coronavirus, the MHV leader RNA sequences were extremely stable and did not evolve significantly during persistent infection. Rather, a 5′ untranslated region (UTR) A-to-G mutation at nt 77 in the genomic RNA emerged by day 56 and accumulated until 50 to 80% of the genome-length molecules retained the mutation by 119 days postinfection. Although other 5′-end mutations were noted, only the nt 77 mutation was significantly associated with viral persistence in vitro. Mutations were also found in the 5′ end of the p28 coding region, but no specific alterations accumulated in genome-length molecules through 119 days postinfection. The 5′ UTR nt 77 mutation resulted in an 18-amino-acid open reading frame (ORF) upstream of the ORF 1a AUG start site. By in vitro translation assays, the small ORF was not translated into detectable product but the mutation significantly enhanced translation of the downstream p28 ORF about 2.5-fold. Variant viruses, containing either the nt 77 A-to-G mutation (V16-ATG$^+$) or wild-type sequences at this locus (V1-ATG$^-$), were isolated at 119 days postinfection. The variant viruses replicated more efficiently than wild-type virus and were extremely cytolytic in DBT cells, suggesting that the A-to-G mutation did not encode a nonlytic or attenuated phenotype. Consistent with the in vitro translation results, a significant increase (~3.5-fold) in p28 expression was also observed with the mutant virus (V16-ATG$^+$) in DBT cells compared with that in wild-type controls. These data indicate that MHV persistence was significantly associated with mutation and evolution in the 5′-end UTR which enhanced the translation of the ORF 1a and potentially ORF 1b polyproteins which function in virus transcription and replication.

Mouse hepatitis virus (MHV), a member of the family *Coronaviradae*, contains a 32-kb single-stranded, nonsegmented, positive-sense genomic RNA that is bound in a helical nucleocapsid structure constructed from multiple bound copies of a 60-kDa basic protein, N (77, 80). The nucleocapsid is surrounded by a lipid envelope bearing three or four structural glycoproteins, including a 180-kDa–90-kDa peplomer glycoprotein (S), a 23-kDa membrane glycoprotein (M), and a 10.5-kDa SM glycoprotein (41, 87). Some strains of MHV contain a 65-kDa hemagglutinin-esterase glycoprotein (55, 76), which has an esterase activity similar to the receptor-destroying enzyme of influenza C virus (85), and a hemagglutinin activity (63, 85). The MHV genomic RNA contains 8 to 10 open reading frames (ORFs). The 5′-most 22 kb of the genomic RNA contain two large ORFs, designated ORF 1a (encoding 440 kDa) and ORF 1b (encoding 310 kDa). Expression of ORF 1b occurs by a ribosomal frameshifting mechanism (15). While the function of the ORF 1a and ORF 1b polyproteins is uncertain, the ORF 1a product contains membrane-rich domains, cysteine-rich domains, and papaine and poliovirus 3C-like protease motifs. The ORF 1b product contains metal-binding domains, helicase, and RNA polymerase sequence motifs, and temperature-sensitive mutants mapping in ORF 1b contain defects in positive- and negative-strand RNA synthesis (7, 14, 15, 31, 34, 52, 63, 73, 78). ORF 1a is probably expressed as a large precursor which is subsequently processed into several viral proteins, including a 220-kDa and an N-terminal 28-kDa protein (6, 78).

The RNA-dependent RNA polymerase directs the synthesis of both full-length and subgenomic-length mRNAs which are arranged in a nested set structure from the 3′ end of the genome (20, 49, 50, 53, 66). All MHV mRNAs also contain a leader RNA sequence at the 5′ end which is derived from the 5′ end of the genome (8, 9, 49). In addition, transcriptionally active full-length and subgenomic-length negative strands which act as templates for the synthesis of the equivalently sized mRNAs are present in infected cells (71, 73, 75). Several discontinuous-transcription models have been proposed to explain the presence of leader RNA sequences in the mRNA and antileaders in the negative-stranded RNA, including the leader-primed transcription, transcription attenuation, and looping-out models (8, 9, 56, 71, 73).

Although MHV and other coronaviruses readily initiate persistent infections in vitro and in vivo, the mechanism by which these viruses establish and maintain a persistent infection is unclear (10, 29, 39, 47, 64, 81). In MHV, previous studies have suggested that virus evolution and mutation result in the production of attenuated temperature-sensitive, cold-sensitive, small-plaque, and fusion-defective viral variants during persistent infection (35, 37, 42, 81), but the function of these virus variants in the establishment or maintenance of MHV persis-

* Corresponding author. Phone: (919) 966-3895. Fax: (919) 966-2089.

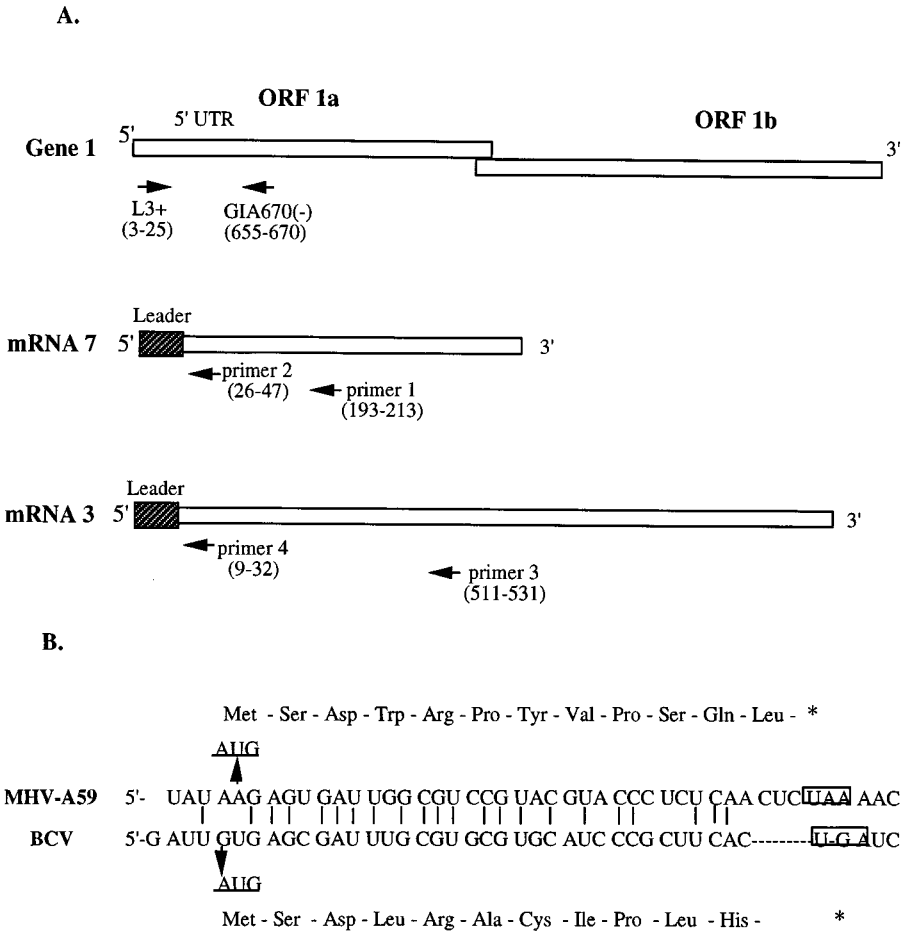

FIG. 1. Cloning strategy and structures of the 5′ end of the MHV-A59 genome, mRNA 3, and mRNA 7. The 5′ end of the MHV genome was cloned by using specific oligomers encompassing the first 670 nt in the genomic RNA. For cloning the 5′ leader of mRNAs 7 and 3, primers 1 and 3 were used to synthesize a cDNA from each mRNA. The internal 3′ primers 2 and 4 were used with the 5′-G-tailed anchor primer for PCR amplification as described in Materials and Methods (A). The comparison of the MHV-A59 and BCV leader RNA sequences reveals that an A-to-U mutation at position 5 could produce an intraleader ORF in MHV-A59 (B).

tence is not clear. During persistent infection with bovine coronavirus (BCV), a group II coronavirus similar to MHV, mutations and evolution in the BCV leader RNA resulted in an intraleader ORF which potentially attenuated the translation of downstream ORFs in each BCV mRNA (38). Unfortunately, little information is available concerning the molecular mechanisms by which MHV and other coronaviruses persist and evolve in vitro and in vivo. We have studied the evolution of the MHV-A59 genome during persistent infection in DBT cells. In contrast to findings in BCV, the MHV leader RNA sequences were extremely stable and did not evolve significantly during persistent infection. Rather, MHV persistence was significantly associated with mutation and evolution in the 5′ untranslated region (UTR) which enhanced translation of the downstream ORF 1a p28 polyprotein in the MHV genome-length RNA.

MATERIALS AND METHODS

Virus, cell lines, and preparation of viral RNA. MHV-A59 was used throughout the course of the studies. Virus was propagated and plaqued in DBT cells as previously described (74). Persistently infected cultures of DBT cells were established by infection at a multiplicity of infection (MOI) of 5 with MHV-A59. After acute cytolytic infection, cells that survived infection (<5%) were cultured into stably infected cell lines that continuously released infectious virus. All cell lines were cultured and passaged under identical treatment conditions in minimum essential medium containing 5% fetal calf serum and 3% newborn calf serum, supplemented with 5% tryptose phosphate broth and 1% penicillin and streptomycin. Intracellular RNA was extracted from acutely and persistently infected cells with RNA STAT-60 reagents (total RNA-mRNA isolation reagent) following the manufacture's directions (Tel-TEST "B," Inc., Friendwood, Tex.).

Cloning and sequencing the 5′ leader RNA on MHV mRNAs. For cloning and sequencing the 5′ leader RNA of mRNAs 3 and 7, the 5′ RACE system kit (GIBCO-BRL) was used throughout the course of these studies. Primer 1 (5′-GCCAGAAAACAAGGAGTAATG-3′), which was complementary to nucleotides (nt) 193 to 213 in the N gene (nucleocapsid protein), and primer 3 (5′-AAACCCTATAAGCTTATTACC-3′), which was complementary to nt 511 to 531 in the S gene (spike protein), were used as primers to synthesize a cDNA from mRNAs 7 and 3, respectively, with reverse transcriptase (72) (Fig. 1A). After purification of the cDNA and 5′-end tail with dCTP and terminal deoxynucleotidyl transferase as described by the manufacturer, the products were mixed with internal antisense primers (3′ primers) and the 5′-G-tailed anchor primer (5′ primer) for PCR amplification. The internal 3′ primers, encoding sequences spanning nt 26 to 47 in the N gene coding region (5′-CAUCAUCAU CAUAGGAGCTTCTGCCACCGGCAT) (primer 2) or spanning nt 9 to 32 in the S gene coding region (5′-CAUCAUCAUCAUGAGGGCAAAAATAGAA TAAACACG-3′) (primer 4) (Fig. 1A), were used for 25 to 30 PCR cycles (the uracil DNA glycosylase cloning site sequence is underlined in primers 2 and 4). The PCR products were purified from 0.8% agarose gels with a QIAEX gel extraction kit (Qiagen Inc., Chatsworth, Calif.) and then ligated into the pAMP1 vector (Bethesda Research Laboratories). The leader primer $L3^+$ (5′-TAAGAG TGATTGGCGTCCGTACG-3′), containing nt 3 to 25 in the leader RNA sequence, was used to identify colonies containing leader RNA sequences (70). The plasmid DNA from positive clones was prepared for sequencing with an INSTA-MINI-PREP kit (5 prime → 3 prime, Inc., Boulder, Colo.) and se-

quenced with the Sequenase version 2.0 DNA sequencing kit (U.S. Biochemicals) with the Sp6 primer.

Sequencing the 5′ end of genomic RNA. To clone the 5′ end of the genomic RNA, cDNA synthesis was first accomplished with reverse transcriptase and random primers (72). Following cDNA synthesis, primers $L3^+$ and GIA 670(−) (5′-AAGTTGAAAGGCCACG-3′), representing nt 655 to 670 in gene 1a, were used for PCR amplification to clone the 5′ end of the MHV-A59 genome (Fig. 1A). The appropriately sized PCR products were cloned into pGEM-T vector (Promega), and positive clones were identified with the $L3^+$ oligomer probe (70). To clone the 5′ end of the genomic RNA from extracellular virus, virions in supernatants were concentrated by ultracentrifugation (40,000 rpm) for 2 h in a Beckman 70TI rotor and virion RNA was extracted with RNA STAT-60 reagents. All sequence analysis was performed with the PC Gene program (IntelliGenetics, Inc., Mountain View, Calif.) as previously described (63).

In vitro transcription, translation, and immunoprecipitation. Two MHV-A59 5′-end genomic clones, A59 G1A-2, derived from input virus at 6 h postinfection, and P16 G1A-16, isolated from persistently infected DBT cells at 56 days postinfection, were chosen for in vitro translation studies. These clones contain nt 3 through 670 at the 5′ end of the genome and should encode a truncated 17-kDa N-terminal fragment of the ORF 1a p28 protein. P16 G1A-16 differed from A59 G1A-2 by a single mutation of A to G at nt 77 in the 5′ UTR. To increase efficiency of p28 protein translation from transcripts derived from these clones, a portion of the leader sequences (nt 3 to 24) was deleted by *Aat*II and *Sna*BI digestion. Following Klenow fill-in and ligation, plasmids A59 G1A-2-L^- and P16 G1A-16-L^- were linearized with *Pst*I and used for in vitro transcription and translation studies.

To detect the putative 1.9-kDa intra-UTR ORF peptide, the A59 G1A-2 and P16 G1A-16 plasmids were linearized by *Nar*I digestion, which cleaves the 5′ UTR at nt 181 downstream of the termination codon from the wild-type and mutant 5′ intra-UTR ORFs. Prior to in vitro transcription, digested plasmids were isolated from 0.8% agarose gels with the QIAEX gel extraction kit (Qiagen Inc.).

Transcripts were generated from 1 μg of the linear DNA template in the presence of 5 mM 7mG(5′)ppp(5′)G cap structure analog (New England Biolabs) by T7 RNA polymerase runoff transcription as described by the manufacturer (Promega). The DNA templates were removed by digestion with RNase-free DNase (10 U; Stratagene), and the transcripts were purified by phenol-chloroform and chloroform extraction (twice) and precipitated with 2 to 3 volumes of ethanol. One microgram of capped in vitro-transcribed RNA was translated in rabbit reticulocyte lysates (Promega) containing 180 mM potassium acetate, 1.5 mM magnesium acetate, and a 1 mM concentration of each amino acid except methionine. [^{35}S]methionine (1,000 mCi/mmol; Amersham) was added at 20 μCi/50 μl of reaction mix, and the reaction mixtures were incubated for 90 min at 30°C. Reactions without RNA transcripts were used as a control. Translation products were analyzed by electrophoresis on sodium dodecyl sulfate (SDS)–18 or 15% polyacrylamide gels as described elsewhere (70).

Immunoprecipitation was performed with α-p28 (anti-p28 serum), kindly provided by Susan Baker, Loyola University (6). Briefly, in vitro-translated products were diluted to 1 ml in radioimmunoprecipitation assay buffer (50 mM Tris [pH 7.4], 0.3 M NaCl, 4 mM EDTA, 0.5% Triton X-100, 0.1% SDS) and incubated with 4 μl of α-p28 with top-to-bottom inversion at 4°C overnight. Following the addition of 50 μl of protein A-Sepharose (Sigma), the reaction mix was incubated for an additional 2 h at 4°C and subsequently washed four times with 1 ml of radioimmunoprecipitation assay buffer. The immunoprecipitated proteins were denatured at 100°C for 4 min in Laemmli loading buffer, and the protein A-Sepharose beads were removed by centrifugation at 14,000 rpm for 5 min in an Eppendorf centrifuge. The proteins were analyzed by electrophoresis on SDS–15% polyacrylamide gels (70), fixed in 5% methanol and 7% acetic acid solution for 30 min, and then soaked overnight in a 10% acetic acid and 1.7% glycerol solution. The gels were impregnated with Enlightening (Amersham), dried, and exposed to Kodak X-ray film at −70°C.

Isolation of virus variants, virus growth curves, and detection of intracellular viral RNA. Virus variants were collected at 119 days postinfection from persistently MHV-A59-infected cultures. Individual viruses were plaque purified twice on DBT cells as previously described, and stock viruses were grown in DBT cells (74). Intracellular RNA was extracted from infected DBT cells by using RNA STAT-60 at 6 h postinfection. Following cDNA synthesis, the 5′ end of the genomic RNA was amplified by PCR using the $L3^+$ and G1A 670(−) primers, and PCR products were cloned and sequenced to identify variants (V-ATG^+) that contained the A-to-G mutation at the 5′-end UTR or that had the wild-type sequence at this locus (V-ATG^-). Variant viruses V16-ATG^+ and V1-ATG^- were chosen for future study.

After isolation and identification of virus variants, cultures of DBT cells were infected at a MOI of 5 for 1 h at room temperature with wild-type and variant viruses. The inoculum was removed, and samples were harvested at different times postinfection and stored at −70°C for plaque assay. Intracellular RNA was also isolated at different times postinfection, and equivalent amounts of extracted RNA were bound to a nitrocellulose filter and hybridized with N gene cDNA subclone IBI 76N probe (74). The ^{32}P-radiolabeled DNA probe was synthesized with a random primer DNA labeling system (GIBCO-BRL). After the filters were exposed to Kodak X-ray film, the dots were localized, excised, and counted. To further quantitate levels of viral mRNA synthesis, cultures of cells (5×10^5) were incubated overnight in 90% phosphate-free minimum essential medium and inoculated with MHV-A59 or V16-ATG^+ at a MOI of 10 for 1 h. The infected cultures were incubated in 99% phosphate-free medium for 6 h, treated with 10 μg of actinomycin D per ml at 3 h postinfection, and radiolabeled with 300 μCi of $^{32}P_i$ per ml from 6 to 7 h postinfection. Intracellular RNAs were extracted as previously described (73). Radiolabeled RNAs were separated on 0.9% agarose gels, dried, and exposed to Kodak X-ray film. Levels of each mRNA were quantitated by the AMBIS radioanalytic imaging system (Ambis, San Diego, Calif.).

Immunoprecipitation of p28 translation products from whole-cell lysates. The preparation of whole-cell lysates and immunoprecipitation of p28 translation products synthesized in vivo were performed as described by Denison et al. (24). Briefly, DBT cells were infected with MHV-A59 or V16-ATG^+ (an nt 77 mutant virus) in 60-mm-diameter petri dishes at a MOI of 10. After the virus inoculum was removed, the cells were incubated in methionine- and cysteine-free Eagle's minimum essential medium containing 2% fetal calf serum. Actinomycin D was added at 3 h postinfection (final concentration, 10 μg/ml), and polypeptides were labeled with [^{35}S]methionine-cysteine (Tran^{35}S-label; ICN) at a concentration of 200 μCi per plate. The cultures were radiolabeled at 5 h postinfection for 2 h. Then radiolabel was removed, the cells were washed twice with 150 mM Tris (pH 7.4) and lysed with 300 μl of 1% Nonidet P-40 lysis solution (1% Nonidet P-40, 1% sodium deoxycholate, 150 mM NaCl, 10 mM Tris, pH 7.4), and the nuclei were removed by centrifugation at 13,000 rpm for 10 min at 4°C in an Eppendorf centrifuge. The supernatant (200 μl) was immunoprecipitated with α-p28 antiserum, and 100 μl of the supernatant was incubated with A1.10, an anti-M protein monoclonal antibody obtained from John Fleming, University of Wisconsin (30). The antibodies were first bound to protein A-Sepharose beads by rocking at 4°C for 2 h and washed three times with the lysis solution containing 0.1% SDS. After immunoprecipitation at 4°C overnight, the supernatants were discarded and the beads were washed four times with alternating high- and low-salt solutions (the lysis solution containing 0.1% SDS and either 150 mM or 1 M NaCl). After rinsing, the proteins were separated by electrophoresis on SDS–15% polyacrylamide gels, and the gels were fixed and dried as described in Materials and Methods. Gels were scanned with an AMBIS radioanalytical imaging system for 12 h, and individual protein bands were imaged and quantitated. The quantity of p28 expression was first standardized to the level of M gene expression and statistically analyzed by using the standard deviation ± the Student *t* test.

Statistical tests. To determine if individual mutations were significantly associated with persistence in vitro, the one- and two-tailed Fisher exact tests were performed (69). Chi-square analysis for trend (biostatistic program Epi Info 6; Centers for Disease Control and Prevention, Atlanta, Ga., and World Health Organization, Geneva, Switzerland) was also used to determine whether a specific mutation is increased in successive groups compared with the baseline level.

RESULTS

Establishment of persistently infected DBT cells. Inoculation of MHV-A59 into DBT cells rapidly results in an acute cytolytic infection in which >95% of the cells are destroyed within 16 h postinfection. The surviving cells replicated to confluence over a 3- to 4-day period (42), and cultures continuously shed infectious virus at titers approaching 10^6 PFU/ml through 119 days postinfection. About 15 to 30% of the cells were positive for viral antigen as detected by an immunofluorescence assay with polyclonal or monoclonal sera, and all viral mRNAs were expressed through 119 days postinfection. The detailed characterization of MHV gene expression and transcription in these cultures will be reported at a later date. In this study, we have examined the evolution of the leader RNA

TABLE 1. Evolution of the 5′-end leader RNA sequence in mRNAs 3 (S gene) and 7 (N gene) during persistent infection

Time postinfection	No. of clones without the mutation[a]/no. of sequenced clones	
	N mRNA	S mRNA
6 h (A59 wild type)	15 (6)/15	15 (4)/15
35 days	21/21	13 (3)/13
105 days	14 (2)/14[b]	12 (4)/12[c]

[a] Numbers in parentheses indicate the number of clones with truncated first and/or second bases.

[b] One clone with a U-to-A mutation at nt 49.

[c] One clone with a G-to-A mutation at nt 25.

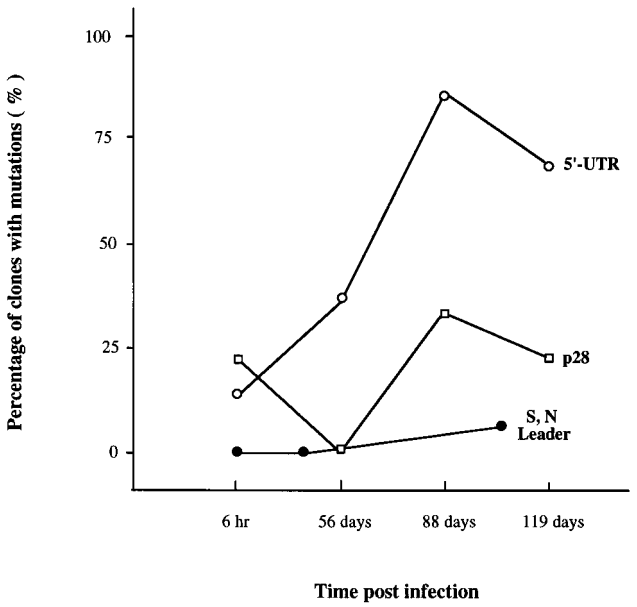

FIG. 2. Evolution of the MHV-A59 leader RNA, p28, and 5′ UTR sequences during persistent infection. Cultures of cells were infected with MHV-A59, and intracellular RNA was isolated at 6 h or 35, 56, 88, 105, or 119 days postinfection. The 5′ ends of mRNAs 7, 3, and 1 were cloned and sequenced. The percentages of the clones containing mutations were shown. S, N Leader, mutations found in leader sequence of the S (mRNA 3) and N (mRNA 7) subgenomic RNAs; 5′-UTR and p28, mutations found in the 5′ UTR and p28 coding region, respectively.

sequences, 5′ UTR, and ORF 1a p28 protein during persistent MHV-A59 infection.

Intraleader ORFs are absent during persistent MHV-A59 infection. It has been suggested that mutations within the 5′ leader RNA of BCV mRNAs function in maintaining persistence in vitro by attenuating translation of downstream ORFs in each mRNA (38). Since MHV-A59 and BCV mRNAs have relatively similar 5′-end leader RNA sequences, an A-to-U point mutation at nt 5 could result in a similar intraleader ORF in MHV-A59 (Fig. 1B). To address this question, the full-length leader RNA sequences of mRNAs 3 and 7 were cloned and sequenced with the 5′ RACE system. Intracellular RNA was isolated at 6 h, 35 days, and 105 days postinfection. Following cDNA synthesis and PCR amplification of the 5′ ends of mRNA 3 and 7 as described in the Materials and Methods, individual clones were isolated and sequenced.

In contrast to findings reported during persistent BCV infection, no 5′-terminal leader mutations were evident in the MHV-A59 mRNAs until 105 days postinfection (Table 1). At 105 days postinfection, only 7 and 8.3% of clones from mRNAs 7 and 3 contained leader RNA mutations (1 of 14 and 1 of 12 clones, respectively) (Fig. 2). One mRNA 7 clone had a U-to-A mutation at nt 49, while an mRNA 3 clone had a G-to-A mutation at nt 25. Neither mutation resulted in intraleader ORFs (Table 1). Interestingly, the extensive polymorphism and deletion noted at the 5′ end of BCV mRNAs were not detected in the MHV-A59 mRNAs, although several clones contained a 1- or 2-nt truncation at the 5′ end which was probably associated with premature termination during reverse transcription. Consequently, the MHV-A59 leader RNA sequence and the leader-mRNA junction sequences were extremely stable and did not evolve significantly through the first 105 days postinfection.

Evolution and mutation in the MHV-A59 genomic RNA. Since our data indicated that intraleader mutations and ORFs were not significantly associated with either the establishment or maintenance of MHV persistence in DBT cells through 105 days postinfection, we cloned and sequenced the 5′ end of the genomic RNA because this domain contains critical *cis*- and *trans*-acting sequences which regulate mRNA, genome RNA, and leader RNA synthesis, as well as the expression of the MHV polymerase (5, 8, 48, 88). The 5′-most 670 bp of genomic RNA were cloned by reverse transcriptase and PCR amplification using two 5′-end-specific primers, $L3^{+}$ and G1A 670(−) (Fig. 1A). Individual plasmid clones containing the 5′ end of MHV-A59 were isolated at 6 h and 56, 88, and 119 days postinfection. An A-to-G mutation at nt 77 was first detected at 56 days postinfection in 1 of 19 clones (Fig. 3A). This mutation created an ORF encoding 16 amino acids (aa) in the 5′ UTR of the genomic RNA. Interestingly, the new ATG start site at nt 75 enlarged the preexisting small ORF (encoding 8 aa) between nt 99 and 125 in wild-type virus (Fig. 3B). In addition to this mutation, other changes were also noted at the 5′ end of the genome in a small number of clones at different

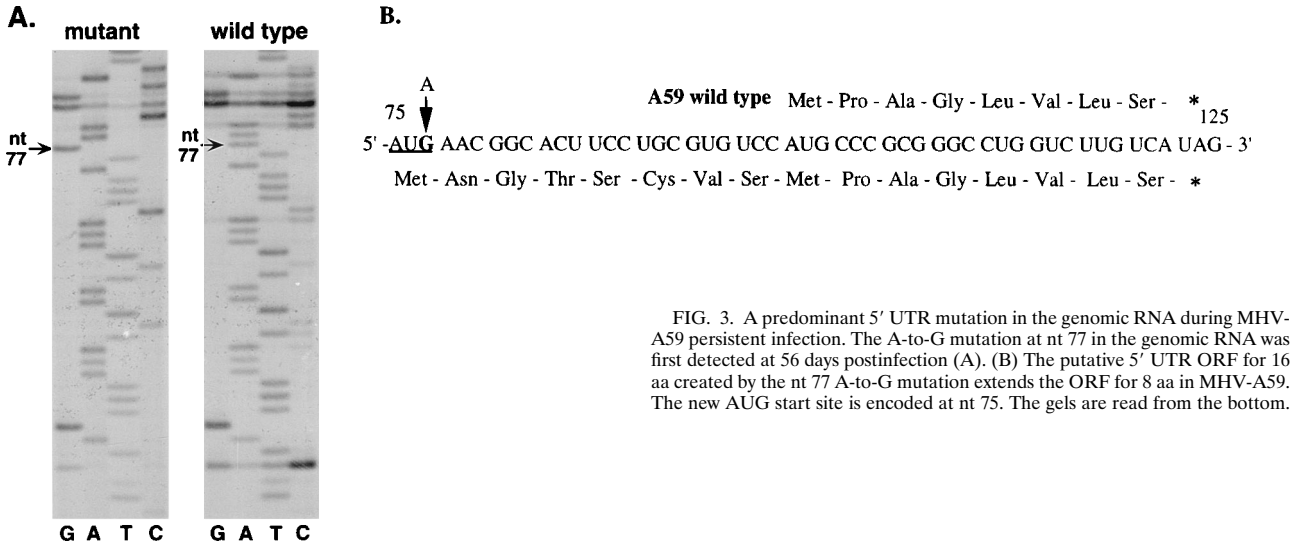

FIG. 3. A predominant 5′ UTR mutation in the genomic RNA during MHV-A59 persistent infection. The A-to-G mutation at nt 77 in the genomic RNA was first detected at 56 days postinfection (A). (B) The putative 5′ UTR ORF for 16 aa created by the nt 77 A-to-G mutation extends the ORF for 8 aa in MHV-A59. The new AUG start site is encoded at nt 75. The gels are read from the bottom.

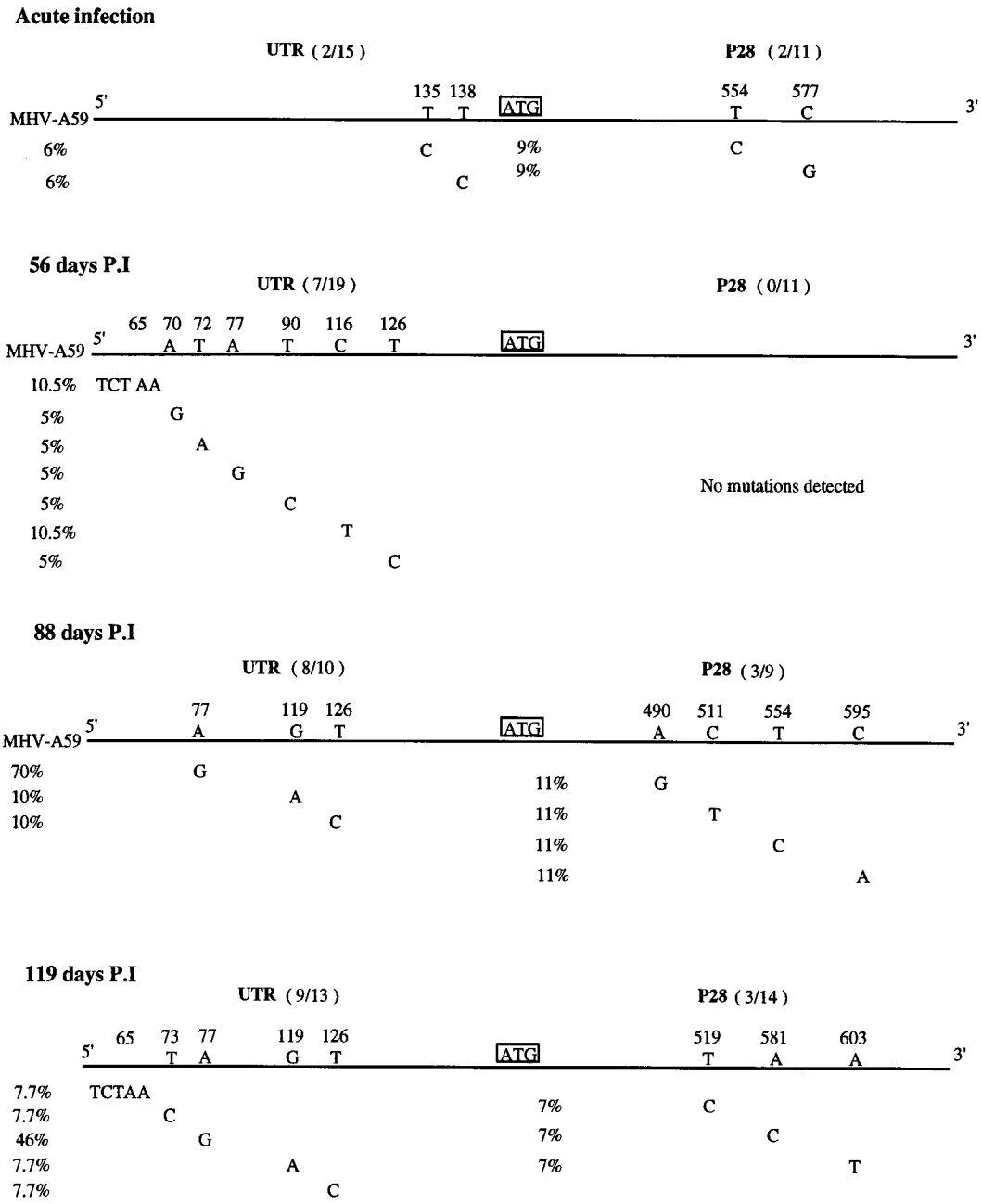

FIG. 4. Evolution and mutation at the 5′ end of the MHV-A59 genome during persistent infection. Intracellular RNA was isolated at 6 h and 56, 88, and 119 days postinfection (P.I) and sequenced as described in Materials and Methods. The numbers of clones containing mutations in the 5′ UTR and p28 coding sequences (in parentheses) and the location of each nucleotide change are shown. The percentages of clones containing a specific mutation are also indicated.

passages. For example, the A-to-G, U-to-A, and U-to-C mutations at nt 70, 72, and 90, respectively, were detected at 56 days postinfection (Fig. 4). However, some evolutionary advantage was clearly associated with the A-to-G mutation at nt 77, because 50 to 80% of the genome-length molecules contained this mutation by 119 days postinfection (Fig. 4). In contrast, most other mutations (7 of 44 clones) were neutral or deleterious and lost with subsequent passage. The only other mutations that appeared to confer some evolutionary advantage were the C-to-U and U-to-C double mutations at nt 119 and 126 seen on days 88 and 119 and a UCUAA insertion at nt 65 seen on days 56 and 119 (Fig. 4). Statistical analysis, however, demonstrated no significant association between these mutations and MHV-A59 persistence (data shown in next section).

Interestingly, the A-to-G mutation is located within potentially important *cis*- and *trans*-acting sequences at the 5′ end of the genome. As previously reported, a relatively stable hairpin loop structure ($\Delta G = -35.2$ kcal [ca. -147 kJ]) may exist at the 5′ end of the MHV genome (63). Compared with the wild type, in the region between nt 72 and 80, the nt 77 mutation did cause some modulation in the putative secondary structure. The overall stability and the structure of the 5′ end of the genome in the mutant virus, however, were very similar to

TABLE 2. Association between a particular mutation and MHV persistence

Position(s) of mutation(s) (nt)	Days postinfection	*P* (Fisher's exact test)
77	56	0.56
77	88	<0.05
77	119	<0.05
119, 126	88	0.40
119, 126	119	0.40
65[a]	56	0.30
65[a]	119	0.47
49 (N gene leader)	105	0.48
25 (S gene leader)	105	0.47

[a] UCUAA insertion.

those of the wild-type virus ($\Delta G = -35.5$ kcal [ca. -149 kJ]) (data not shown).

Molecular evolution of MHV-A59 during persistent infection. Among the RNA viruses, the rate at which mutations become fixed in different portions of the viral genome varies during persistent infection (18, 19, 26). To compare the mutation rates in different portions of the MHV genome during persistent infection, we also sequenced the 5′ end of the p28 nonstructural protein coding region in some of the same clones that contained the 5′-end UTR. The number of mutations in the sequenced p28 coding region was significantly low. During acute infection (6 h postinfection), the numbers of clones containing mutations in both regions were similar: 18% (2 of 11 clones) contained mutations in p28 and 13% (2 of 15 clones) contained mutations in the 5′-end UTR. After passage, the rates at which mutations accumulated in these two regions were significantly different. In p28, no mutations were detected at 56 days postinfection but 30% (3 of 9) and 21% (3 of 14) of the clones contained mutations by 88 and 119 days postinfection, respectively. In contrast, 37% (7 of 19), 80% (8 of 10), and 69% (9 of 13) of the clones contained mutations in the 5′-end UTR at 56, 88, and 119 days postinfection (Fig. 4). Statistical analysis for trend indicated a specific increase in the number of mutations detected within the 5′ UTR ($P < 0.001$) but not for the mutations in the p28 domain ($P < 0.43$) over time. Among the mutations found in the 5′ end of the p28 coding region, 30% were silent and only one (1 of 45 clones sequenced), at position 603 (A to T), resulted in a premature stop codon by 119 days postinfection. No mutations in the p28 coding region appeared to contribute evolutionary advantages, since they did not accumulate through 119 days postinfection. The rate of fixation of mutations was 4.3×10^{-5} to 7.58×10^{-5} and 1.2×10^{-5} to 3.37×10^{-5}/nt/day, and the mutation frequency ranged from 3.3×10^{-3} to 6.7×10^{-3} and 1.2×10^{-3} to 2.96×10^{-3} substitutions per nt in the 5′ UTR and p28 coding regions (8,550 and 6,750 nt sequenced in each region), respectively.

Since infectious clones are not available to evaluate the role of a particular mutation in MHV-A59 persistence, we have used biostatistical techniques to determine if a particular mutation was significantly associated with MHV-A59 persistence in vitro (69). Statistical analysis has clearly demonstrated a strong association ($P < 0.05$) between mutation and evolution at nt 77 in the genomic RNA during MHV-A59 persistence at days 88 and 119 postinfection (Table 2). Similar associations were not detected among other 5′ end genomic mutations on days 56, 88, and 119 postinfection or among mutations detected in p28 ($P > 0.1$). Importantly, statistical analysis for trend also demonstrated a significant increase in the number of clones containing the A-to-G mutation over time ($P < 0.001$) compared with baseline levels. No significant evolution was present within either the leader RNA or intergenic sequences as well ($P > 0.1$). These data indicate that the 5′ UTR A-to-G mutation was significantly associated with the maintenance of the MHV-A59 genome in persistently infected DBT cells.

In vitro translation studies. As the 5′ UTR A-to-G mutation is located near the leader sequence at the 5′ end of the genome, it might alter the virus replication cycle by affecting the transcription of leader RNA or mRNA or altering the efficiency of translation of the genomic RNA. Alternatively, the 5′ UTR ORF may be translated into a small, ~1.9-kDa peptide which modulates the acute cytolytic potential of MHV-A59.

To test whether the intra-UTR ORF is translated into the putative 1.9-kDa product, two clones were translated in rabbit reticulocyte lysates in vitro (Fig. 5A). Clone A59 G1A-2 was isolated from input wild-type A59 acute infection (6 h postinfection), and its sequence was identical to the reported MHV-A59 sequence (63). A putative 8-aa peptide of about 1 kDa is encoded in the 5′-end UTR between nt 99 and 125 in wild-type virus (63). The P16 G1A-16 clone was obtained from persistently infected cells at 56 days postinfection and was identical to clone A59 G1A-2 except for a single A-to-G mutation at nt 77, encoding a potential 16-aa ORF product of about 1.9 kDa between nt 75 and 125 at the 5′ end of the genome. The plasmids were linearized with *Nar*I, which cleaves downstream from the termination codon for the 8- and 16-aa ORF products (nt 181), and in vitro transcription and translation were performed as described in Materials and Methods. No radiolabeled polypeptide of the predicted size for the intra-UTR ORF product (1 or 1.9 kDa) was detected from either A59 G1A-2 or P16 G1A-16 transcripts, suggesting that both ORFs were in a poor context for translation in vitro (data not shown).

We then addressed whether the nt 77 mutation altered the level of p28 protein expression in the in vitro translation assay. As the presence of the leader sequences greatly reduces the efficiency of p28 translation in vitro (4a), a small portion of leader RNA sequences (nt 3 to 23) in both plasmids was deleted by enzymatic digestion to enhance p28 expression. The 5′-truncated plasmids A59 G1A-2-L$^-$ and P16 G1A-16-L$^-$ were linearized with *Pst*I, and equivalent amounts of in vitro transcripts were translated in vitro. In vitro translation of both plasmids resulted in the synthesis of a 17-kDa protein, equivalent in size to the N-terminal 153 aa of p28 that is encoded in each plasmid. Antiserum α-p28, which is directed against the N terminus of p28, immunoprecipitated the 17-kDa product, demonstrating that it contained p28 coding sequences (Fig. 5B). The radioactive protein products were analyzed by gel electrophoresis and quantitated by AMBIS. Compared with that in the MHV-A59 wild-type control, a significant 2.37 ± 0.54-fold (mean ± standard deviation; $n = 3$) increase in p28 expression was observed when the intra-UTR ORF was present, suggesting that this mutation increased the translational efficiency of the MHV-A59 genomic RNA ($P < 0.05$) (Fig. 5B).

Role of the 5′-end UTR mutation in MHV persistence. The accumulation of the 5′-end nt 77 mutation in the MHV-A59 genome by day 56 postinfection suggests that the mutation functions in establishing or maintaining MHV-A59 persistence in vitro. To test this hypothesis, we isolated intracellular viral RNA, extracellular virion RNA, and virion RNA from 12 twice-plaque-purified infectious virus clones at 119 days postinfection. Sequence analysis indicated that the nt 77 mutation

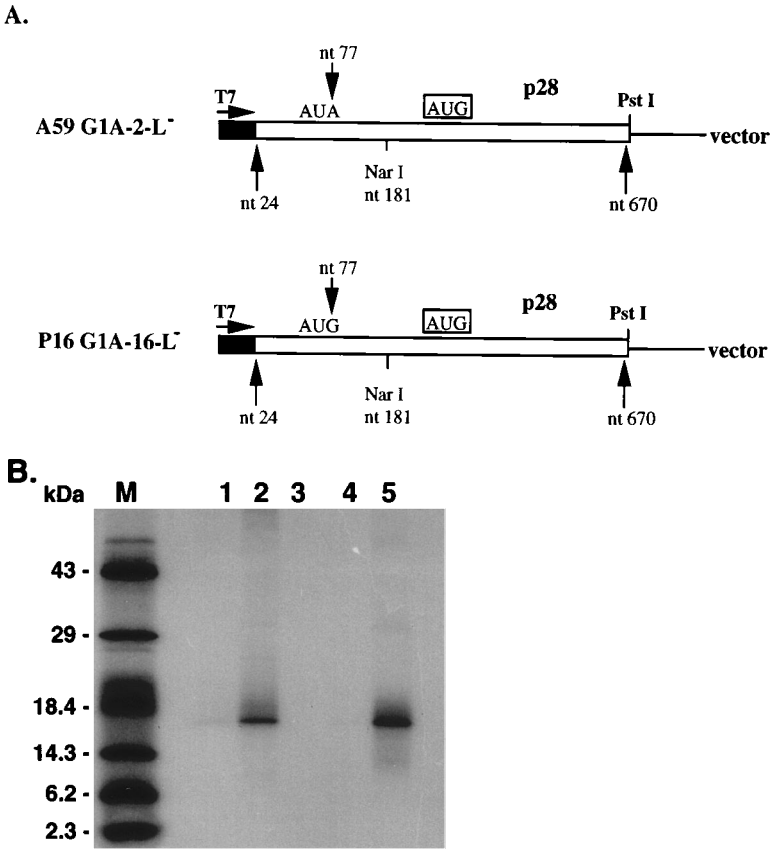

FIG. 5. Effect of the nt 77 A-to-G mutation on the expression of the ORF 1a p28 protein. In vitro translation of transcripts synthesized from the clones depicted in Fig. 1B was performed as described in Materials and Methods. (A) These clones encode the N-terminal 17 kDa of the p28 nonstructural protein. (B) Immunoprecipitation of the truncated p28 in vitro. Lanes 1 and 4, translation products from A59 G1A-2-L$^-$; lanes 2 and 5, translation products from P16 GIA-16-L$^-$; lane 3, no RNA transcripts (control).

was present in 46% (6 of 13) of the cloned intracellular genomic RNAs, 33% (4 of 12) of the cloned extracellular virion RNAs (infectious and noninfectious), and 50% (6 of 12) of the plaque-purified isolates at 119 days postinfection (Table 3). Virus isolates with (V16-ATG$^+$) or without (V1-ATG$^-$) the A-to-G mutation at 119 days postinfection were extremely virulent, fusigenic, and cytolytic and destroyed >99% of the DBT monolayers within 16 h postinfection. Thus, the variant viruses were not more efficient than wild-type virus in establishing a persistent infection in the parental cell lines. These data suggested that neither the A-to-G mutation nor the new 5′-end ORF encoding the putative 16-aa peptide attenuated the cytopathic effect of MHV-A59 or enhanced its ability to establish a persistent infection in vitro. Rather, virus growth curves demonstrated that V16-ATG$^+$ and V1-ATG$^-$ replication was increased compared with that of wild-type virus in DBT cells under identical conditions, suggesting that persistence selected for more-virulent virus variants (Fig. 6A). By 24 h postinfection, V16-ATG$^+$ infection resulted in 123 PFU per cell, compared to 136 PFU per cell for V1-ATG$^-$ and 26 PFU per cell for MHV-A59. Interestingly, V16-ATG$^+$ replication was significantly more efficient at early times in the infection compared with that of MHV-A59 and V1-ATG$^-$ (Fig. 6B). At 6 h postinfection, the production of infectious virus averaged 43.3 PFU per cell for V16-ATG$^+$, 0.06 PFU per cell for MHV-A59, and 0.5 PFU per cell for V1-ATG$^-$. Consistent with this hypothesis, levels of viral intracellular RNA were increased throughout V16-ATG$^+$ infection, as well as V1-ATG$^-$ infection, compared with that in wild-type MHV-A59 infection (Fig. 6B). To provide additional evidence that more-vigorous virus variants evolve during MHV persistence, cultures of DBT cells were infected with MHV-A59 and V16-ATG$^+$ at a MOI of 10 and radiolabeled with $^{32}P_i$ from 6 to 7 h postinfection. Increased levels of mRNA 1 to 7 synthesis were clearly evident in V16-ATG$^+$-infected cultures compared with those in the wild-type control (Fig. 6C). AMBIS scans indicated that the relative percent molar ratio of each mRNA was similar, but V16-ATG$^+$ transcribed about three times more RNA than MHV-A59 at this time postinfection.

To determine whether viral infection was characterized by increased expression of the ORF 1a products in vivo, the levels of p28 expression were monitored during acute MHV-A59 and V16-ATG$^+$ infection in DBT cells. Cultures of the cells were infected and radiolabeled for 2 h with [^{35}S]methionine-cysteine

TABLE 3. Distribution of the nt 77 mutation in cloned intracellular genomic RNAs, extracellular virion RNAs, and plaque-purified isolates at 119 days postinfection

Source of virus	No. of clones with ATG mutation/no. of clones sequenced	% with the mutation
Intracellular	6/13	46
Extracellular	4/12	33
Plaque purified	6/12	50

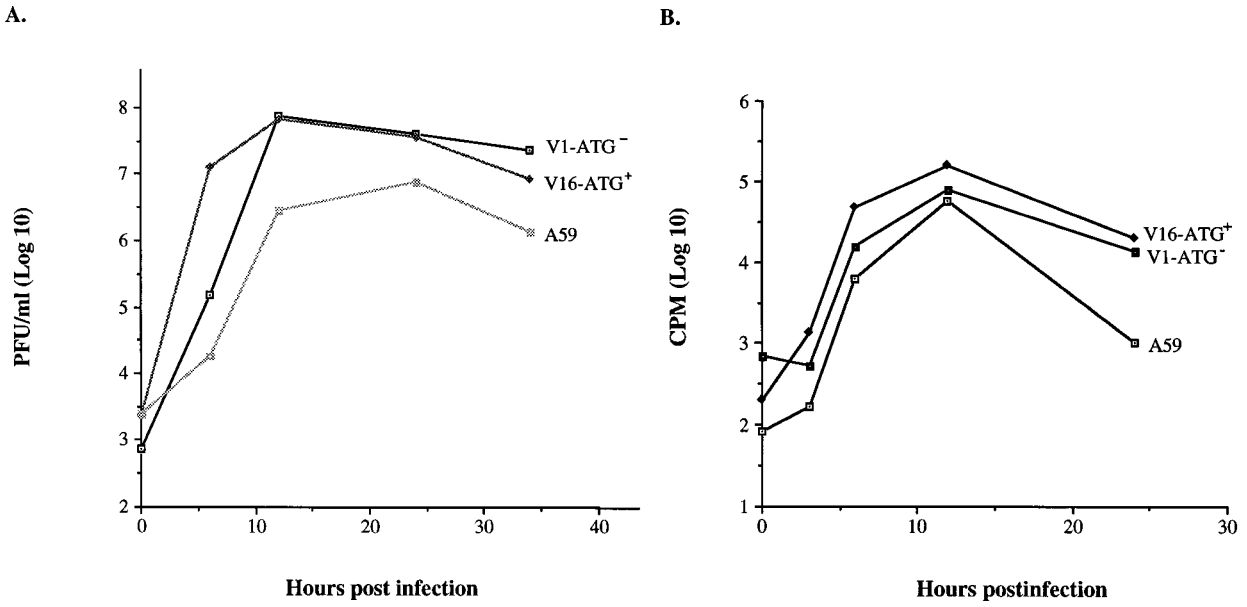

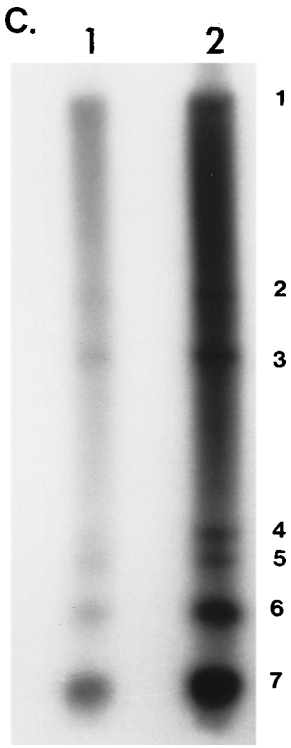

FIG. 6. Replication of MHV-A59 and variant viruses V16-ATG$^+$ and V1-ATG$^-$ in DBT cells. Cultures of cells (3×10^5) were infected with these viruses at a MOI of 5. Intracellular RNA was also isolated at different times postinfection, bound to nitrocellulose filters, and probed with ^{32}P-radiolabeled MHV-A59 N gene cDNA. The dots were localized, excised, and counted after the filters were exposed to Kodak X-ray film, and the amount of RNA was reported as counts per minute (B). The inoculum was removed, and samples were taken at different times postinfection. Infectious virions were enumerated by plaque assay (A). (C) Levels of RNA synthesis were determined by radiolabeling MHV-A59- or V16-ATG$^+$-infected cultures at 6 to 7 h postinfection. Lane 1, MHV-A59; lane 2, V16-ATG$^+$. Viral mRNAs are labeled from 1 to 7.

at 5 h postinfection. The MHV p28 and M proteins were immunoprecipitated with p28 antiserum or monoclonal antibody to the M glycoprotein and separated on SDS–15% polyacrylamide gels as described in Materials and Methods. The amount of p28 expression was quantitated by AMBIS scans relative to M gene expression. Consistent with the in vitro translation results, a 3.21 ± 1.03-fold increase in p28 expression was observed with the mutant virus V16-ATG$^+$ compared with that in the control (Fig. 7) ($P < 0.05$, $n = 4$). Thus, these data were consistent with the notion that the 5′-end UTR A-to-G mutation in V16-ATG$^+$ was likely associated with increased ORF 1a p28 protein expression. In these gels, increased levels of p28 labeling compared with those of the M protein were likely due to the presence of threefold more cysteine and methionine residues in p28 and the early labeling times. Similar results have been observed previously (24).

DISCUSSION

The molecular mechanisms of RNA virus persistence in vitro and in vivo have received considerable attention over the past few decades (4), leading not only to the elucidation of viral gene functions but also to the identification of important sites of virus-host interaction which modulate cell injury and death (1, 12, 19, 23, 25, 58, 68, 79). While coronaviruses readily establish persistent infections in vitro, they are predominately associated with acute infections in humans and animals (59). The recent identification of persisting neurotropic coronaviruses in the human, mouse, and primate central nervous systems (17, 29, 61, 64, 84), coupled with the unique genetic organization and replication strategy of these viruses (48), suggests that novel virus-host interactions evolve to modulate the cytolytic potential of these viruses.

Although many groups have established persistent coronavirus infections in vitro, the precise mechanisms by which this cytoplasmic RNA virus establishes and maintains a persistent infection are uncertain. It is also unclear how rapidly the viral genome evolves under these conditions. Coronaviruses, like other positive-polarity RNA viruses, have high mutation rates probably caused by the lack of proofreading capabilities in the RNA polymerase (26). MHV polymerase error rates estimated by reversion frequencies of temperature-sensitive mutants

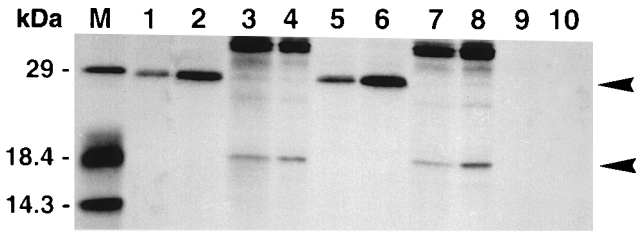

FIG. 7. Immunoprecipitation of p28 and M protein from DBT cells infected with MHV-A59 and V16-ATG$^+$ variant virus. Duplicate cultures of cells were infected at a MOI of 10 and incubated in methionine-cysteine-free media. Polyproteins were labeled with 200 μCi of [^{35}S]methionine-cysteine per plate, immunoprecipitated, and separated on SDS–15% polyacrylamide gels. Lanes 1 and 5, p28 protein from MHV-A59-infected cells; lanes 2 and 6, p28 protein from V16-ATG$^+$-infected cells; lanes 3 and 7, M protein from MHV-A59-infected cells; lanes 4 and 8, M protein from V16-ATG$^+$-infected cells; lanes 9 and 10, uninfected cells with α-p28 antisera or A1.10 anti-M protein monoclonal antibody; lane M, molecular weight markers. Arrowheads indicate p28 (28-kDa) and M (23-kDa) proteins.

range from 10^{-3} to 10^{-5} substitution per site (31), very similar to mutation frequencies of 10^{-3} to 10^{-4} substitution per nt measured during MHV persistence through 119 days postinfection. While these values may be slightly elevated because of high error rates associated with the reverse transcriptase and *Taq* polymerases, these values are very similar to rates measured for other positive-stranded RNA viruses, including transmissible gastroenteritis virus (27, 40, 86). The majority of evolutionary changes detected in this study probably represented the random fixation of selectively neutral or nearly neutral mutations under continued selection (46). Deleterious mutations were lost, but rare advantageous mutations (A to G at nt 77) rapidly spread through the population, readily explaining the increased percentage of genomic clones that contained the 5′-end mutation at later times. In MHV, the p28 protein and leader RNA evolved at much lower rates compared with the 5′ UTR, consistent with the notion that viral sequences evolve at different rates during persistent infection (18, 19, 33). Like influenza virus evolution in the face of host immune selection, our data also suggest that MHV undergoes positive Darwinian selection during persistent infection (28).

Persistence of RNA viruses in vitro is associated with gene evolution, mutations in critical domains that function in the normal virus replication cycle, and/or the coevolution of host cells that resist viral cytopathology (2, 4, 12, 23, 25, 45, 58, 68). During BCV infection, persistence was associated with the evolution of 5′-end intraleader RNA mutations which attenuated the translation of downstream ORFs in each mRNA (38). Unfortunately, the 5′-end mutation, extensive hypervariability, and polymorphism in the BCV leader RNA sequences did not develop during MHV persistence. Rather, through 105 days postinfection, the MHV leader RNA sequences and intergenic start sites were extremely stable and highly conserved. As the clones containing leader RNA sequences were identified by the L3$^+$ (nt 3 to 25) probe, our method may not have detected extreme polymorphisms in 5′-end leader RNA if nt 3 to 25 sequences in the leader RNA were deleted or significantly altered. However, clones containing point mutations and intraleader ORFs should have been detected. While it is possible that intraleader mutations evolve later during MHV persistence, such mutations were evident within 4 days after BCV infection and subsequently accumulated with passage. These data suggest that the establishment and maintenance of MHV persistence are mediated by different host-virus interactions that are uncoupled from the presence of intraleader polymorphisms, mutations, and translation-attenuating intraleader ORFs. In addition, if leader-body junction sequences encode critical *cis*- and *trans*-acting elements that are required for virus transcription as predicted by the leader-primed and transcription attenuation models for discontinuous transcription of coronavirus RNAs, stable leader-body junction sequences should be maintained during persistent infection (39, 54, 71, 73, 75, 88). Since leader RNA sequences in mRNA and genome evolve at similar low rates, these data suggest that these sequences are critical elements in virus transcription.

The difference in the evolution of BCV and MHV mRNAs is intriguing and suggests that different mechanisms of persistence occur among the group II coronaviruses. Interestingly, BCV infection in HRT cells is noncytolytic, dramatically different from the extremely cytolytic MHV infection in DBT cells (38). It is well established that the host cell environment dramatically regulates the cytopathic potential of MHV. For example, MHV infection in LM-K cells or primary mouse glial cells occurs in the absence of significant cytopathology, fusion, and cell killing (51, 60). In contrast, the infection in 17 Cl-1, L2, and DBT cells is extremely cytolytic (37). While additional studies must be performed, the most likely explanation for these different findings is that viral strains and host cell genotypes exert different selection pressures on the coronavirus genome, resulting in the evolution and accumulation of distinct mutations that initiate and maintain viral persistence (1, 13, 22, 25). In support of this hypothesis, it has been reported that organ-specific selection of viral variants has been demonstrated during chronic lymphocytic choriomeningitis virus infection in carrier mice (3) and that the host cell environment imposes significant evolutionary constraints in the selection of precise silent mutations in the poliovirus genome (13).

While intraleader ORFs did not develop in mRNAs from persistently infected DBT cells, MHV persistence was significantly associated with the evolution and accumulation of a specific A-to-G mutation that resulted in the appearance of a new ORF for 16 aa in the 5′ UTR of the genomic RNA. The selection for precise mutations is not without precedent and has been reported during poliovirus and foot-and-mouth disease virus (FMDV) persistence (13, 26). Persistent noncytolytic MHV infection in primary mouse glial cells also selects for fusion-defective MHV-A59 variants that contain precise mutations in the spike glycoprotein gene (35). In our study, the nt 77 A-to-G mutation was significantly associated with increased expression of the ORF 1a p28 polyprotein in vitro, suggesting that the 5′-UTR mutation enhances expression of the genes at the 5′ end of the MHV genome. The 5′ end of the MHV genome contains two large ORFs, designated ORF 1a and ORF 1b, which are probably translated into two large polyproteins of 440 and 330 kDa by a ribosomal frameshifting mechanism (11, 15, 52). These large polyproteins are then processed by viral and/or host proteases into the MHV polymerase proteins and other proteins functioning in RNA synthesis (52). Since the p28 protein is encoded at the N terminus of ORF 1a, enhanced p28 expression is likely associated with an increased expression of all viral gene 1 products, including the putative viral RNA polymerase. Consonant with these findings, virus replication, RNA synthesis, and gene expression were also increased in variant viruses containing the mutation, suggesting that the 5′-end mutation contributed to MHV persistence by increasing polymerase gene expression. Additional genetic alterations, however, must also occur in the genomes of viruses isolated during persistent infection, since variants lacking the A-to-G mutation also replicated more efficiently than wild-type virus. Definitive structure-function analysis of the 5′-end mutation and element and ORF must be accessed upstream of

reporter genes to definitively ascertain its affects on secondary structure and in the stimulation of translation. Similar quantitative assays have been reported in picornavirus (57).

The 5′ UTR in many positive-strand RNA viruses has been demonstrated not only to regulate viral protein expression but also to function in the replication and transcription of viral positive-stranded RNA (16, 44, 54, 57, 67, 79). Systemic movement of a hordeivirus is regulated by 5′-end substitutions in the genome (65). A single nucleotide mutation in the ribosome entry site of FMDV has been demonstrated to enhance cap-independent translation in vitro two- to fourfold (57). During acute MHV infection, a 13-nt element (UCUAAUCCAAA CA) containing the UCUAA pentanucleotide repeat within leader RNA sequences enhances the translation of viral mRNAs. Enhanced translation of viral mRNAs may also require an interaction between specific viral proteins and this pentanucleotide repeat as well (82). Since the A-to-G mutation resides within a similar pentanucleotide repeat element (UAUAA to UAUGA) just 3′ to the leader RNA pentanucleotide repeat motifs in the genomic RNA, this alteration may enhance translation of genome-length molecules by a similar *cis*-recessive mechanism (82). The 5′ UTR mutation might also enhance MHV replication by regulating the level of subgenomic mRNA synthesis, since the mutation resides within a 9-nt domain (UUUAUAAA) that has been suggested to regulate the initial synthesis of the viral subgenomic mRNAs by promoting or attenuating leader RNA switching between templates (88). We have not, however, detected any significant difference in the relative percent molar ratio of the V16-ATG$^+$ or wild-type mRNAs during infection. Alternatively, in wild-type virus, a putative small 8-aa peptide which might function to downregulate expression of the ORF 1a and 1b polyproteins is encoded in the MHV-A59 5′ UTR. Since the nt 77 mutation expands this ORF product to a 16-aa peptide, this may alter the regulation of MHV polymerase gene expression. This mechanism does not, however, explain the increased replication efficiency of variant viruses lacking the A-to-G mutation in DBT cells, and in vitro translation studies suggest that the putative 1.9-kDa protein is poorly expressed at best. Thus, the most likely explanation for the nt 77 mutation's function in MHV persistence is that it enhances the persistence of the MHV genome by enhancing translation of the ORF 1a and 1b polyproteins. Consistent with this hypothesis, the nt 77 mutation appears to alter the secondary structure of the 5′ end of the genomic RNA, and similar enhancing mutations have been described in piconavirus (57).

Viral persistence likely involves alterations in critical host-virus interactions which initiate a persistent infection and subsequently lead to selection for mutations which maintain the persistent state by attenuating or enhancing virus replication or by altering host susceptibility to infection (19, 57, 58). Distinct mechanisms which function in the establishment and maintenance of a persistent poliovirus, FMDV, and reovirus infection have been described elsewhere (3, 12, 25, 58). Like the BCV intraleader ORF (38), the MHV 5′-end mutation probably functions in the maintenance of a persistent infection, since it does not evolve until after 56 days postinfection. Thus, it seems likely that other genetic changes in the virus or host must evolve to initially establish and maintain a persistent MHV infection. The evolution of a specific 5′-end enhancing mutation as well as other potential mutations which probably contributes to the maintenance of MHV persistence by increasing the efficiency of virus replication and virulence is surprising in view of the well-documented evidence demonstrating that the attenuation of viral gene functions or downregulation of specific viral genes is the principle mechanism limiting cell killing (1, 4, 43, 62). Our findings are not, however, unique, since variant viruses, which were more cytolytic and replicated more efficiently than the wild type have been isolated from persistent reovirus and FMDV cultures (1, 23, 58). Persistently coxsackie A9 virus-infected HeLa cell cultures also selected for viruses with increased virulence, while echovirus 6 variant viruses which could not replicate in the parental cells evolved during persistent infection (21, 32, 83). Functional alterations that favored measles virus persistence have also been demonstrated (36). Since the evolution of virulent virus variants in persistent cultures seems to be related to the coevolution of host cell variants that resist the cytopathic effects of wild-type viruses, these data suggest that MHV persistence is mediated by similar coevolutionary mechanisms in vitro (22, 23, 58).

ACKNOWLEDGMENTS

We thank Boyd Yount, Jr., for excellent technical assistance.

This research was supported by a research grant from the National Institutes of Health (AI 23946) and a fellowship from the Public Health Service (5 T32 A107151-16) to W.C. This research was conducted during the tenure of an established investigator award from the American Heart Association (89-0193) to R.S.B.

REFERENCES

1. **Ahmed, R., M. Canning, R. S. Kauffman, A. H. Sharpe, J. V. Hallum, and B. N. Fields.** 1981. Role of the host cell in persistent viral infection: coevolution of L cells and reovirus during persistent infection. Cell **25:**325–332.
2. **Ahmed, R., and B. N. Fields.** 1982. Role of the S4 gene in the establishment of persistent reovirus infection in L cells. Cell **28:**605–612.
3. **Ahmed, R., C. S. Hahn, T. Somasundaram, L. Villarette, M. Matloubian, and J. H. Strauss.** 1991. Molecular basis of organ-specific selection of viral variants during chronic infection. J. Virol. **65:**4242–4247.
4. **Ahmed, R., and J. G. Stevens.** 1990. Viral persistence, p. 241–265. *In* B. N. Fields and D. M. Knipe (ed.), Virology, 2nd ed. Raven Press, New York.

4a. **Baker, S.** Personal communication.

5. **Baker, S. C., and M. M. C. Lai.** 1990. An *in vitro* system for the leader-primed transcription of coronavirus mRNAs. EMBO J. **9:**4173–4179.
6. **Baker, S. C., C.-K. Shieh, L. H. Soe, M.-F. Chang, D. M. Vannier, and M. M. C. Lai.** 1989. Identification of a domain required for autoproteolytic cleavage of murine coronavirus gene A polyprotein. J. Virol. **63:**3693–3699.
7. **Baric, R. S., K. Fu, M. C. Schaad, and S. A. Stohlman.** 1990. Establishing a genetic recombination map for murine coronavirus strain A59 complementation groups. Virology **177:**646–656.
8. **Baric, R. S., S. A. Stohlman, and M. M. C. Lai.** 1983. Characterization of replicative intermediate RNA of mouse hepatitis virus: presence of leader RNA sequences on nascent chains. J. Virol. **48:**633–640.
9. **Baric, R. S., S. A. Stohlman, M. K. Razavi, and M. M. C. Lai.** 1985. Characterization of leader-related small RNAs in coronavirus infected cells: further evidence for leader-primed mechanism of transcription. Virus Res. **3:**19–33.
10. **Baybutt, H. N., H. Wege, M. J. Carter, and V. Ter Meulen.** 1984. Adaptation of coronavirus JHM to persistent infection of murine Sac(−) cells. J. Gen. Virol. **65:**915–924.
11. **Bonilla, P. J., A. E. Gorbalenya, and S. R. Weiss.** 1994. Mouse hepatitis virus strain A59 RNA polymerase gene ORF 1a: heterogeneity among MHV strains. Virology **198:**736–740.
12. **Borzakian, S., T. Couderc, Y. Barbier, G. Attal, I. Pelletier, and F. Colbere-Garapin.** 1992. Persistent poliovirus infection: infection establishment and maintenance involve distinct mechanisms. Virology **186:**398–408.
13. **Borzakian, S., I. Pelletier, V. Calvez, and F. Colbere-Garapin.** 1993. Precise missense and silent point mutations are fixed in the genomes of poliovirus mutants from persistently infected cells. J. Virol. **67:**2914–2917.
14. **Boursnell, M. E. G., T. D. K. Brown, I. J. Foulds, P. F. Green, F. M. Tomley, and M. M. Binns.** 1987. Completion of the sequence of the genome of the coronavirus avian infectious bronchitis virus. J. Gen. Virol. **68:**57–77.
15. **Bredenbeek, P. J., C. J. Pachuk, A. F. H. Noten, J. Charite, W. Luytjes, S. R. Weiss, and W. J. M. Spaan.** 1990. The primary structure and expression of the second open reading frame of the polymerase gene of the coronavirus MHV-A59; a highly conserved polymerase is expressed by an efficient ribosomal frameshifting mechanism. Nucleic Acids Res. **18:**1825–1832.
16. **Brown, E. A., S. P. Day, R. W. Jansen, and S. M. Lemon.** 1991. The 5′ nontranslated region of hepatitis A virus RNA: secondary structure and elements required for translation in vitro. J. Virol. **65:**5828–5838.
17. **Burks, J. S., B. L. Devald, L. D. Jakovsky, and J. C. Gerdes.** 1980. Two coronaviruses isolated from central nervous system tissue of two multiple sclerosis patients. Science **209:**933–934.

18. **Cattaneo, R., A. Schmid, D. Eschle, K. Baczko, V. ter Meulen, and M. A. Billeter.** 1988. Biased hypermutation and other genetic changes in defective measles viruses in human brain infections. Cell **55:**255–265.
19. **Cattaneo, R., A. Schmid, P. Spielhofer, K. Kaelin, K. Baczko, V. ter Meulen, J. Pardowitz, S. Flanagan, K. B. Rima, S. A. Udem, and M. A. Billeter.** 1989. Mutated and hypermutated genes of persistent measles viruses which caused lethal human brain diseases. Virology **173:**415–425.
20. **Cheley, S., R. Anderson, M. J. Cupples, E. C. M. L. Chan, and V. L. Morris.** 1981. Intracellular murine hepatitis virus-specific RNAs contain common sequences. Virology **112:**596–604.
21. **Crowell, R. L., and J. T. Syverton.** 1961. The mammalian cell-virus relationship. VI. Sustained infection of HeLa cells by coxsackie B3 virus and effect of superinfection. J. Exp. Med. **113:**419–435.
22. **de la Torre, J. C., S. de la Luna, J. Diez, and E. Domingo.** 1989. Resistance to foot-and-mouth disease virus mediated by *trans*-acting cellular products. J. Virol. **63:**2385–2387.
23. **de la Torre, J. C., E. Martínez-Salas, J. Diez, A. Villaverde, F. Gebauer, E. Rocha, M. Dávila, and E. Domingo.** 1988. Coevolution of cells and viruses in a persistent infection of foot-and-mouth disease virus in cell culture. J. Virol. **62:**2050–2058.
24. **Denison, M. R., P. W. Zoltick, S. A. Hughes, B. Giangreco, A. L. Olson, S. Perlman, J. L. Leibowitz, and S. R. Weiss.** 1992. Intracellular processing of the N-terminal ORF 1a proteins of the coronavirus MHV-A59 requires multiple proteolytic events. Virology **189:**274–284.
25. **Dermody, T. S., M. L. Nibert, D. Wetzel, X. Tong, and B. N. Fields.** 1993. Cells and viruses with mutations affecting viral entry are selected during persistent infections of L cells with mammalian reoviruses. J. Virol. **67:**2055–2063.
26. **Domingo, E., and J. J. Holland.** 1994. Mutation rate and rapid evolution of RNA viruses, p. 161–184. *In* S. S. Morse (ed.), The evolutionary biology of viruses. Raven Press, New York.
27. **Enjuanes, L., C. Sanchez, F. Gebauer, A. Mendez, J. Dopazo, and M. L. Ballesteros.** 1993. Evolution and tropism of transmissible gastroenteritis coronavirus, p. 35–42. *In* H. Laude and J. F. Vautherot (ed.), Advances in experimental medicine and biology. Plenum Press, New York.
28. **Fitch, W. M., J. M. E. Leiter, X. Li, and P. Palese.** 1991. Positive Darwinian evolution in human influenza A viruses. Proc. Natl. Acad. Sci. USA **88:**4270–4274.
29. **Fleming, J. O., J. J. Houtman, H. Alaca, H. C. Hinze, D. McKenzie, J. Aiken, T. Bleasdale, and S. Baker.** 1994. Persistence of viral RNA in the central nervous system of mice inoculated with MHV-4, p. 327–332. *In* H. Laude and F. J. Vautherot (ed.), Coronaviruses. Plenum Press, New York.
30. **Fleming, J. O., S. A. Stohlman, R. C. Harmon, M. M. C. Lai, J. A. Frelinger, and L. P. Weiner.** 1983. Antigenic relationships of murine coronaviruses: analysis using monoclonal antibodies to JHM (MHV-4) virus. Virology **131:** 296–307.
31. **Fu, K. S., and R. S. Baric.** 1994. Map locations of mouse hepatitis virus temperature-sensitive mutants: confirmation of variable rates of recombination. J. Virol. **68:**7458–7466.
32. **Gibson, J. P., and V. F. Righthand.** 1985. Persistence of echovirus 6 in cloned human cells. J. Virol. **54:**219–223.
33. **Gojobori, T., E. N. Moriyama, and M. Kimura.** 1990. Molecular clock of viral evolution, and the neutral theory. Proc. Natl. Acad. Sci. USA **87:**10015–10018.
34. **Gorbalenya, A. E., E. V. Koonin, A. P. Donchenko, and V. M. Blinov.** 1989. Coronavirus genome: prediction of putative functional domains in the nonstructural polyprotein by comparative amino acid sequence analysis. Nucleic Acids Res. **17:**4847–4861.
35. **Hingley, S. T., J. L. Gombold, E. Lavi, and S. R. Weiss.** 1994. MHV-A59 fusion mutants are attenuated and display altered hepatotropism. Virology **200:**1–10.
36. **Hirano, A., M. Ayata, A. H. Wang, and T. C. Wong.** 1993. Functional analysis of matrix proteins expressed from cloned genes of measles virus variants that cause subacute sclerosing panencephalitis reveals a common defect in nucleocapsid binding. J. Virol. **67:**1848–1853.
37. **Hirano, N., N. Goto, S. Makino, and K. Fujiwara.** 1981. Persistent infection with mouse hepatitis virus JHM strain in DBT cell culture, p. 301–308. *In* V. ter Meulen, S. Siddell, and H. Wege (ed.), Biochemistry and biology of coronaviruses. Plenum Press, New York.
38. **Hofmann, M. A., S. D. Senanayake, and D. A. Brian.** 1993. A translation-attenuating intraleader open reading frame is selected on coronavirus mRNAs during persistent infection. Proc. Natl. Acad. Sci. USA **90:**11733–11737.
39. **Hofmann, M. A., P. B. Sethna, and D. A. Brian.** 1990. Bovine coronavirus mRNA replication continues throughout persistent infection in cell culture. J. Virol. **64:**4108–4114.
40. **Holland, J., K. Spindler, F. Horodyski, E. Grabau, S. Nichol, and S. Vande-Pol.** 1982. Rapid evolution of RNA genomes. Science **215:**1577–1585.
41. **Holmes, K. V.** 1990. Coronaviridae and their replication, p. 841–856. *In* B. N. Fields and D. M. Knipe (ed.), Virology. Raven Press, New York.
42. **Holmes, K. V., and J. N. Behnke.** 1981. Evolution of a coronavirus during persistent infection in vitro, p. 287–299. *In* V. ter Meulen, S. Siddell, and H. Wege (ed.), Biochemistry and biology of coronavirus. Plenum Press, New York.
43. **Huang, D. D., M. A. Nugent, J. K. Rosenberger, and T. J. Schnitzer.** 1987. Association of avian reovirus M and S with viral behavior in vivo. I. Viral persistence. Avian Dis. **31:**438–445.
44. **Jang, S. K., A. Davies, R. J. Kaufman, and E. Wimmer.** 1989. Initiation of protein synthesis by internal entry of ribosomes into the 5′ nontranslated region of encephalomyocarditis virus RNA in vivo. J. Virol. **63:**1651–1660.
45. **Kauffman, R. S., R. Ahmend, and B. N. Fields.** 1983. Selection of a mutant S1 gene during reovirus persistent infection of L cells. Virology **131:**79–87.
46. **Kimura, M.** 1989. The neutral theory of molecular evolution and the world view of the neutralists. Genome **31:**24–31.
47. **Knobler, R. L., P. W. Lampert, and M. B. A. Oldstone.** 1982. Virus persistence and recurring demyelination produced by a temperature-sensitive mutant of MHV-4. Nature (London) **298:**279–280.
48. **Lai, M. M. C.** 1990. Coronavirus: organization, replication and expression of genome. Annu. Rev. Microbiol. **44:**303–333.
49. **Lai, M. M. C., R. S. Baric, P. R. Brayton, and S. A. Stohlman.** 1984. Characterization of leader RNA sequences of the virion and mRNAs of mouse hepatitis virus, a cytoplasmic virus. Proc. Natl. Acad. Sci. USA **81:** 3626–3630.
50. **Lai, M. M. C., P. R. Brayton, R. C. Arman, C. D. Patton, C. Pugh, and S. A. Stohlman.** 1981. Mouse hepatitis virus A59 messenger RNA structure and genetic localization of the sequence divergence from the hepatotropic strain MHV3. J. Virol. **39:**823–834.
51. **Lavi, E., A. Suzumura, M. Hirayama, M. K. Highkin, D. M. Dambach, D. H. Silberberg, and S. R. Weiss.** 1987. Coronavirus mouse hepatitis virus (MHV)-A59 causes a persistent, productive infection in primary glial cell cultures. Microb. Pathog. **3:**79–86.
52. **Lee, H.-J., C.-K. Shieh, A. E. Gorbalenya, E. V. Koonin, N. La Monica, J. Tuler, A. Bagdzhadzhyan, and M. M. C. Lai.** 1991. The complete sequence (22 kilobases) of murine coronavirus gene 1 encoding the putative proteases and RNA polymerase. Virology **180:**567–582.
53. **Leibowitz, J. L., and S. R. Weiss.** 1981. Murine coronavirus RNA, p. 227–244. *In* V. ter Meulen, S. Siddell, and H. Wege (ed.), Biochemistry and biology of coronaviruses. Plenum Press, New York.
54. **Liao, C.-L., and M. M. C. Lai.** 1994. Requirement of the 5′-end genomic sequence as an upstream *cis*-acting element for coronavirus subgenomic mRNA transcription. J. Virol. **68:**4727–4737.
55. **Luytjes, W., P. J. Bredenbeek, A. F. H. Noten, M. C. Horzinek, and W. J. M. Spaan.** 1988. Sequence of mouse hepatitis virus A59 mRNA 2: indications for RNA recombination between coronavirus and influenza C virus. Virology **166:**415–422.
56. **Makino, S., S. A. Stohlman, and M. M. C. Lai.** 1986. Leader sequences of murine coronavirus mRNAs can be freely reassorted: evidence for the role of free leader RNA in transcription. Proc. Natl. Acad. Sci. USA **83:**4204–4208.
57. **Martinez-Salas, E., J.-C. Saiz, M. Davila, G. J. Belsham, and E. Domingo.** 1993. A single nucleotide substitution in the internal ribosome entry site of foot-and-mouth disease virus leads to enhanced cap-independent translation in vivo. J. Virol. **67:**3748–3755.
58. **Martin Hernandez, A. M., E. C. Carrillo, N. Sevilla, and E. Domingo.** 1994. Rapid cell variation can determine the establishment of a persistent viral infection. Proc. Natl. Acad. Sci. USA **91:**3705–3709.
59. **McIntosh, K.** 1990. Coronaviruses, p. 857–864. *In* B. N. Fields and D. M. Knipe (ed.), Virology, 2nd ed. Raven Press, New York.
60. **Mizzen, L., S. Cheley, M. Rao, R. Wolf, and R. Anderson.** 1983. Fusion resistance decreased infectability as major host cell determinants of coronavirus persistence. Virology **128:**407–417.
61. **Murray, R. S., G.-Y. Cai, K. Hoel, J.-Y. Zhang, K. F. Soike, and G. F. Cabirac.** 1992. Coronavirus infects and causes demyelination in primate central nervous system. Virology **188:**274–284.
62. **Nonoyama, M., Y. Watanabe, and A. F. Graham.** 1970. Defective virions of reovirus. J. Virol. **6:**226–236.
63. **Pachuk, C., P. J. Bredenbeek, P. W. Zoltick, W. J. M. Spaan, and S. R. Weiss.** 1989. Molecular cloning of the gene encoding the putative polymerase of mouse hepatitis coronavirus, strain A59. Virology **171:**141–148.
64. **Perlman, S., G. Jacobsen, L. A. Olson, and A. Afifi.** 1990. Identification of the spinal cord as a major site of persistence during chronic infection with a murine coronavirus. Virology **175:**418–426.
65. **Petty, I. T. D., M. C. Edwards, and A. O. Jackson.** 1990. Systemic movement of an RNA plant virus determined by a point substitution in a 5′ leader sequence. Proc. Natl. Acad. Sci. USA **87:**8894–8897.
66. **Robb, J. A., and C. W. Bond.** 1979. Pathogenic murine coronaviruses. I. Characterization of biological behavior in vitro and virus-specific intracellular RNA of strongly neurotropic JHMV and weakly neurotropic A59 viruses. Virology **94:**352–370.
67. **Rohll, J. B., N. Percy, R. Ley, D. J. Evans, J. W. Almond, and W. S. Barclay.** 1994. The 5′-untranslated regions of picornavirus RNAs contain independent functional domains essential for RNA replication and translation. J. Virol. **68:**4384–4391.
68. **Ron, D., and J. Tal.** 1985. Coevolution of cells and virus as a mechanism for

the persistence of lymphotropic minute virus of mice in L-cells. J. Virol. **55:**424–430.
69. **Rosner, B.** 1990. *In* Fundamentals of biostatistics, p. 336–342. PWS-KENT Publishing Co., Boston.
70. **Sambrook, J., E. F. Fritsch, and T. Maniatis.** 1989. Molecular cloning: a laboratory manual, 2nd ed., p. 11.31, 12.21. Cold Spring Harbor Laboratory Press, Cold Spring Harbor, N.Y.
71. **Sawicki, S. G., and D. L. Sawicki.** 1990. Coronavirus transcription: subgenomic mouse hepatitis virus replicative intermediates function in RNA synthesis. J. Virol. **64:**1050–1056.
72. **Schaad, M. C., and R. S. Baric.** 1993. Evidence for new transcriptional units encoded at the 3′ end of the mouse hepatitis virus genome. Virology **196:** 190–198.
73. **Schaad, M. C., and R. S. Baric.** 1994. Genetics of mouse hepatitis virus transcription: evidence that subgenomic negative strands are functional templates. J. Virol. **68:**8169–8179.
74. **Schaad, M. C., S. A. Stohlman, J. Egbert, K. Lum, K. Fu, T. J. Wei, and R. S. Baric.** 1990. Genetics of mouse hepatitis virus transcription: identification of cistrons which may function in positive and negative strand RNA synthesis. Virology **177:**634–645.
75. **Sethna, H. B., S.-L. Hung, and D. A. Brian.** 1989. Coronavirus subgenomic minus-strand RNAs and the potential for mRNA replicons. Proc. Natl. Acad. Sci. USA **86:**5626–5630.
76. **Shieh, C.-K., H.-J. Lee, K. Yokomori, N. La Monica, S. Makino, and M. M. C. Lai.** 1989. Identification of a new transcriptional initiation site and the corresponding functional gene 2b in the murine coronavirus RNA genome. J. Virol. **63:**3729–3736.
77. **Skinner, M. A., and S. G. Siddell.** 1983. Coronavirus JHM: nucleotide sequence of the mRNA that encodes nucleocapsid protein. Nucleic Acids Res. **15:**5045–5054.
78. **Soe, L. H., C.-K. Shieh, S. C. Baker, M.-F. Chang, and M. M. C. Lai.** 1987. Sequence and translation of the murine coronavirus 5′-end genomic RNA reveals the N-terminal structure of the putative RNA polymerase. J. Virol. **61:**3968–3976.
79. **Stein, S. B., L. Zhang, and R. P. Roos.** 1992. Influence of Theiler's murine encephalomyelitis virus 5′ untranslated region on translation and neurovirulence. J. Virol. **66:**4508–4517.
80. **Stohlman, S. A., R. S. Baric, G. N. Nelson, L. H. Soe, L. M. Welter, and R. K. Deans.** 1988. Specific interaction between the coronavirus leader RNA and nucleocapsid protein. J. Virol. **62:**4288–4295.
81. **Stohlman, S. A., A. Y. Sakaguchi, and L. P. Weiner.** 1979. Characterization of the cold-sensitive hepatitis virus mutants rescued from latently infected cells by cell fusion. Virology **98:**448–455.
82. **Tahara, S. M., T. A. Dietlin, C. C. Bergmann, G. W. Nelson, S. Kyuwa, R. P. Anthony, and S. A. Stolhman.** 1994. Coronavirus translational regulation: leader affects mRNA efficiency. Virology **202:**621–630.
83. **Takemoto, K. K., and K. Habel.** 1959. Virus-cell relationship in a carrier culture of HeLa cells and coxsackie A9 virus. Virology **7:**28–44.
84. **Tanaka, R., Y. Iwasaki, and H. Koprowski.** 1976. Ultrastructural studies of perivascular cuffing cells in multiple sclerosis brain. J. Neurol. Sci. **28:**121.
85. **Vlasak, R., W. Luytjes, W. J. M. Spaan, and P. Palese.** 1988. Human and bovine coronaviruses recognize sialic acid-containing receptor similar to those of influenza C virus. Proc. Natl. Acad. Sci. USA **85:**4526–4529.
86. **Ward, C. D., and J. B. Flanegan.** 1992. Determination of the poliovirus RNA polymerase error frequency at eight sites in the viral genome. J. Virol. **66:**3784–3793.
87. **Yu, X., W. Bi, S. R. Weiss, and J. L. Leibowitz.** 1994. Mouse hepatitis virus gene 5b protein is a new virion envelope glycoprotein. Virology **202:**1018–1023.
88. **Zhang, X., C.-L. Liao, and M. M. C. Lai.** 1994. Coronavirus leader RNA regulates and initiates subgenomic mRNA transcription both in *trans* and in *cis*. J. Virol. **68:**4738–4746.